Supporting Information

Metastable Quantum Dot for Photoelectric Devices via Flash-induced One-step Sequential Self-formation

Tae Hong Im[a[+]], Chul Hee Lee[a[+]], Jong Chan Kim[d], Shinho Kim[b], Mina Kim[a], Cheol Min Park[b], Han Eol Lee[a], Jung Hwan Park[a], Min Seok Jang[b], Doh C. Lee[c], Sung-Yool Choi[b], Hee Seung Wang[a], Hu Young Jeong[d], Duk Young Jeon[a*] and Keon Jae Lee[a*]*

[*] Corresponding author at: Department of Materials Science and Engineering, Korea Advanced Institute of Science and Technology (KAIST), 291 Daehak-ro, Yuseong-gu, Daejeon, 34141, Republic of Korea.

*E-mail: hulex@unist.ac.kr (H. Y. J), dyjeon@kaist.ac.kr (D. Y. J.)
and keonlee@kaist.ac.kr (K. J. L.),

[+] These authors contributed equally to this work.

Keywords: Light-material interaction, metastable quantum dot, sequential self-formation, localized-surface plasmon, photoelectric device

This file includes

- Fig. S1 to Fig. S17
- Table. S1 and Table. S2
- Supporting Information References

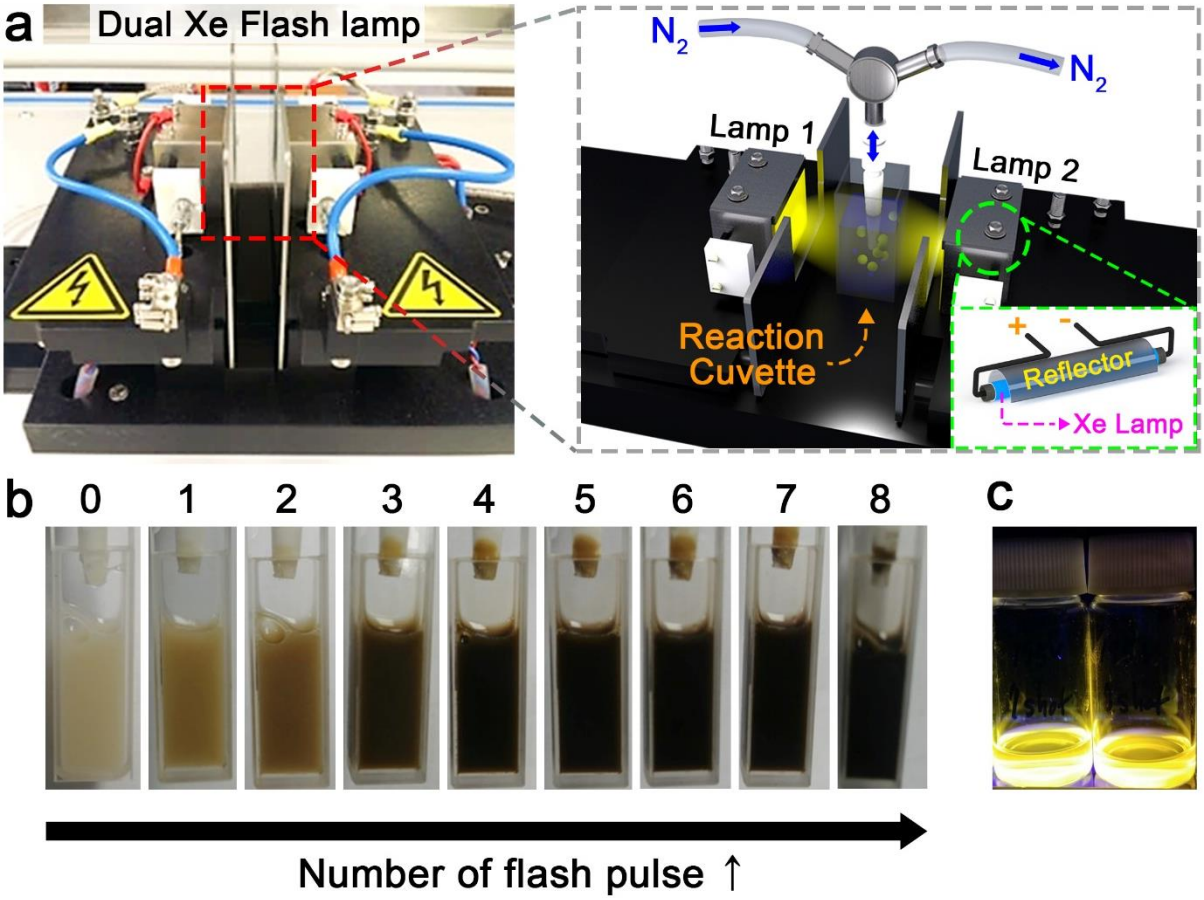

Fig. S1. (a) Flash-induced meta-QD synthesis system using dual-channel xenon flash lamp. The intensive flash-light was irradiated on precursor-filled reaction cuvette using both lamps (Lamp 1 and Lamp 2) with parabolic optical reflector. (b) Color change of reaction solution after multiple irradiation of flash pulses (0 ~ 8 times). Between each pulse illumination, the reaction solution was mixed by voltex mixer. (c) The final metastable Ag, ZnS: α-In_2S_3 QDs dispersed in chloroform after washing and purification process.

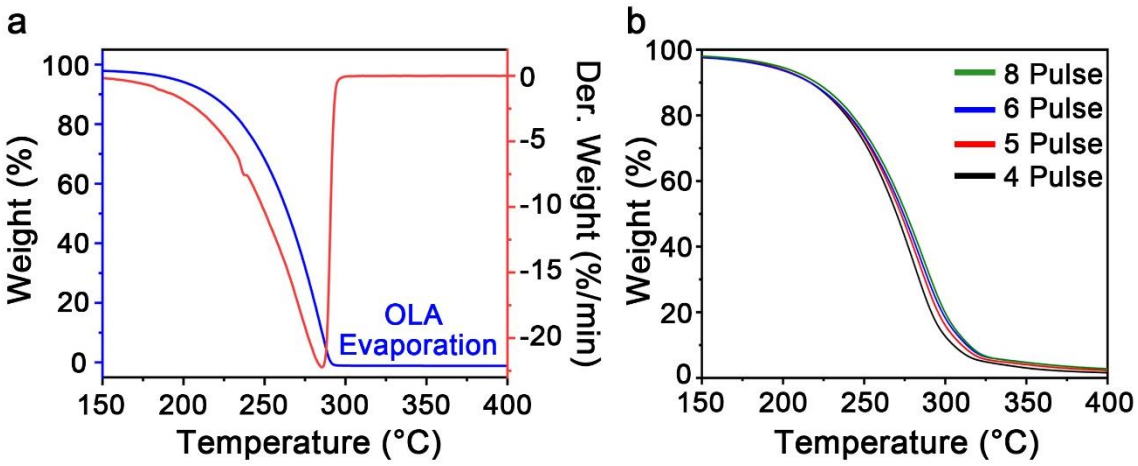

Fig. S2. (a) Thermo-gravimetric (TG) analysis of pure OLA solvent. (b) TG analysis of reaction solution after multi-pulse irradiation. All samples were measured based on steady-temperature increment rate of 30 ℃*/min*).

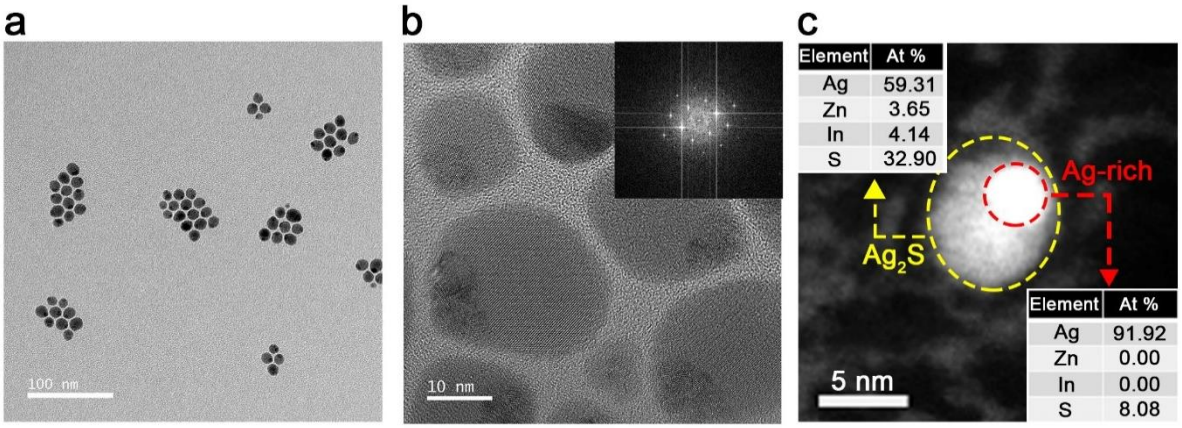

Fig. S3. (a), (b) bright field image of HR-TEM for intermediate Ag_2S/Ag NPs after 1 ~ 2 pulse irradiation on reaction solution. The average diameter of Ag_2S/Ag NPs was about 15 nm. The inset of Fib. S3b presents the diffraction patterns of Ag_2S/Ag NP. (c) STEM-EDS element analysis of single Ag_2S/Ag NPs. The Ag-rich metallic phase (red-colored region) and semiconductive Ag_2S phase (yellow-colored region) were successfully verified.

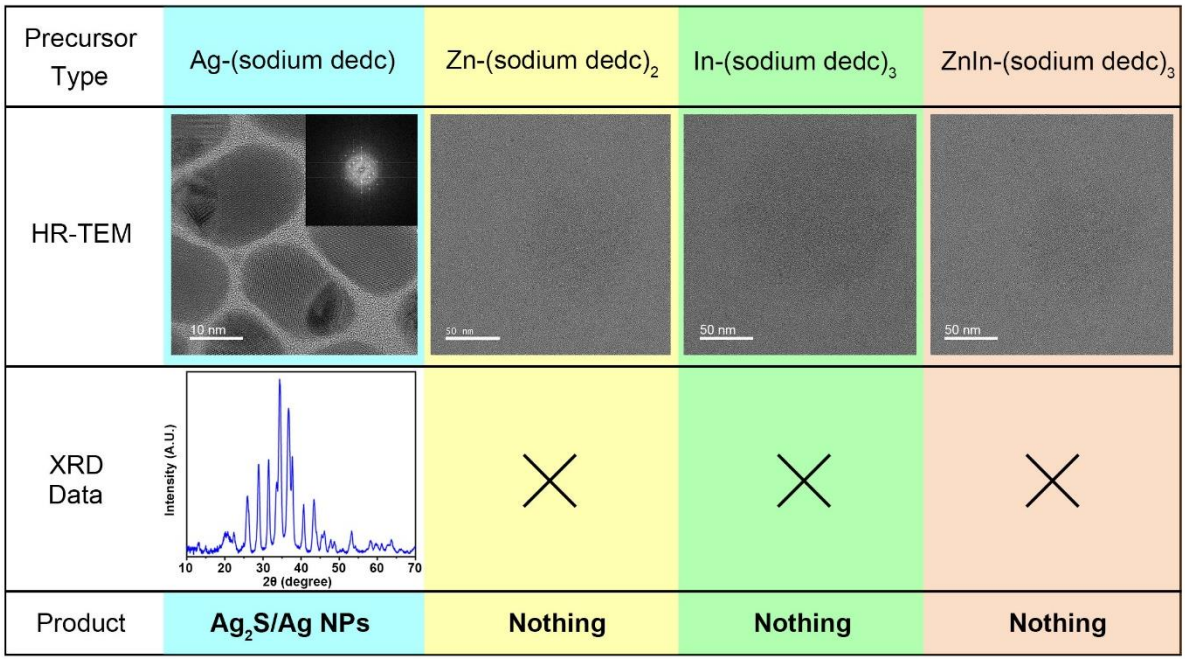

Fig. S4. Control experiments of light-induced QD synthesis using four different metal-organosulfur complex precursors including Ag-(sodium dedc), Zn-(sodium dedc)$_2$, In-(sodium dedc)$_3$ and ZnIn-(sodium dedc)$_3$. Only synthesis using Ag-(sodium dedc) precursor displayed formation of silver sulfide (Ag_2S/Ag) NPs. The XRD data of the silver sulfide product presented the monoclinic crystal structure [S1].

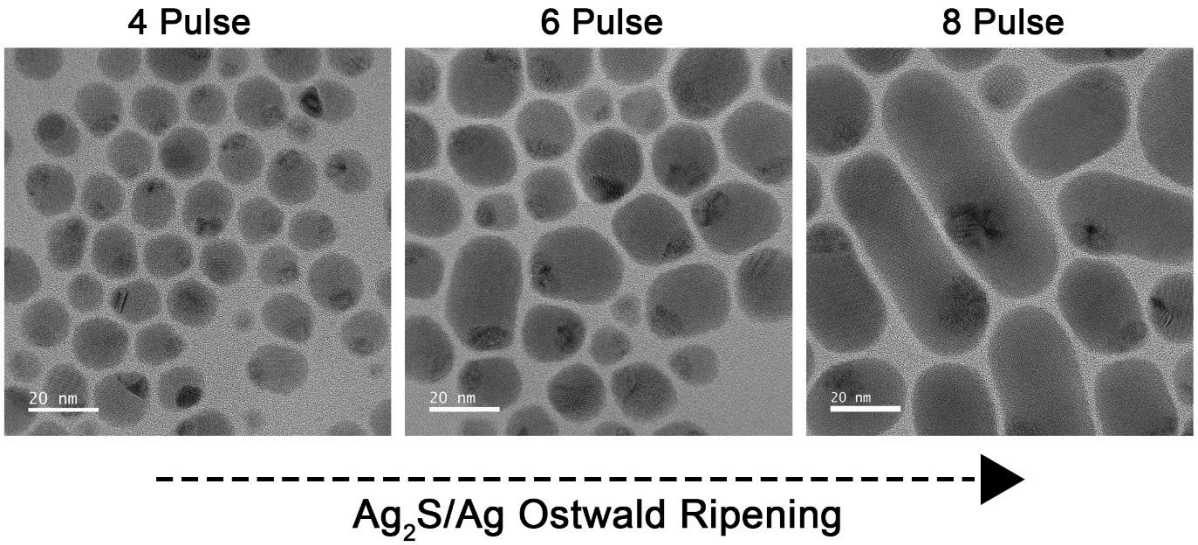

Fig. S5. Bright field HR-TEM image of intermediate silver sulfide NPs which were synthesized from $In3^{+}$-deficient precursor. Without In^{3+} in reaction solution, the Ag_2S/Ag became bigger in size by Ostwald ripening according to the number of irradiated flash pulses.

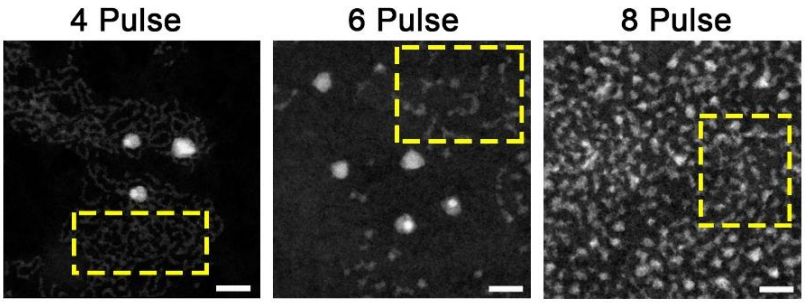

Element (at%)	4 Pulse	6 Pulse	8 Pulse
In	28.8	31.7	39.7
S	58.2	45.3	25.2
Ag	5.6	11.1	16.0
Zn	7.4	11.9	19.1

Ag, Zn increase

Fig. S6. STEM-EDS analysis to verify the gradual increment of Ag-doping and ZnS-passivation on the metastable α-In_2S_3 QDs according to the number of pulse irradiation. The right graph presents that the amounts of Ag and Zn in QD were increased by Ag-doping and Zn-passivation, respectively.

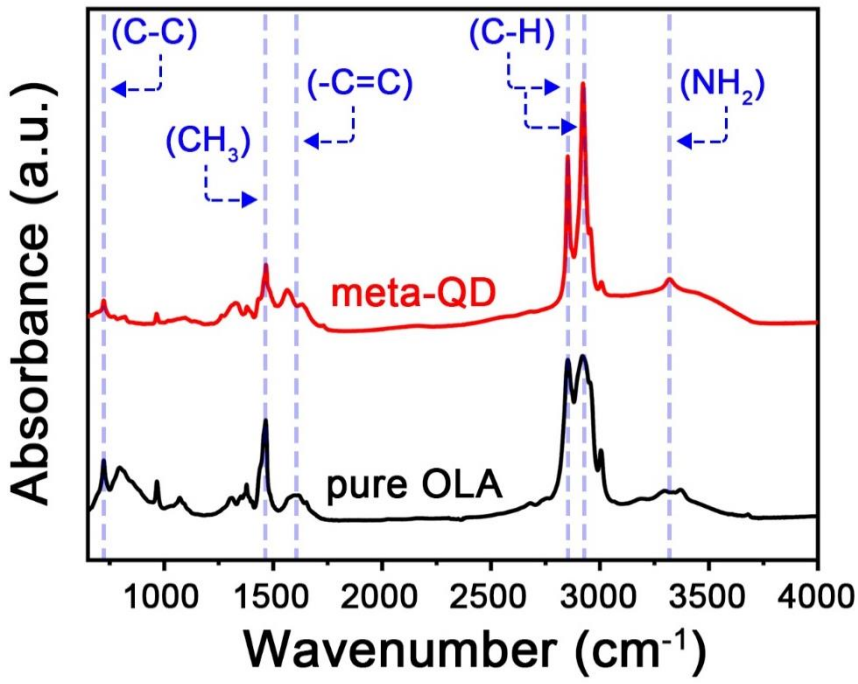

Fig. S7. FT-IR spectrum of pure OLA solvent and Ag, ZnS: α-In_2S_3 QDs in 600 ~ 4000 cm^{-1} region. The Attachment of OLA ligand on metastable QDs was successfully proved by comparing FT-IR spectrum. The various vibrational modes (symmetric stretching, asymmetric stretching and bending) of OLA functional groups (C-C, CH_3, -C=C, C-H, NH_2, etc.) were matched to the characteristic absorption bands of metastable QDs.

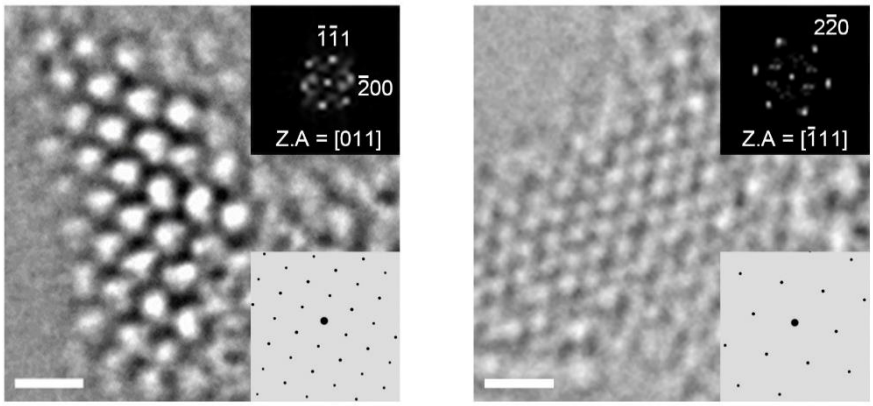

Fig. S8. HRTEM images, corresponding FFT patterns (upper insets) and electron diffraction simulations (lower insets) with different zone axis including [011] and [$\bar{1}$11] presenting cubic crystal structure of light-induced metastable Ag, ZnS: α-In_2S_3 QD. The white scale bars are 0.5 nm.

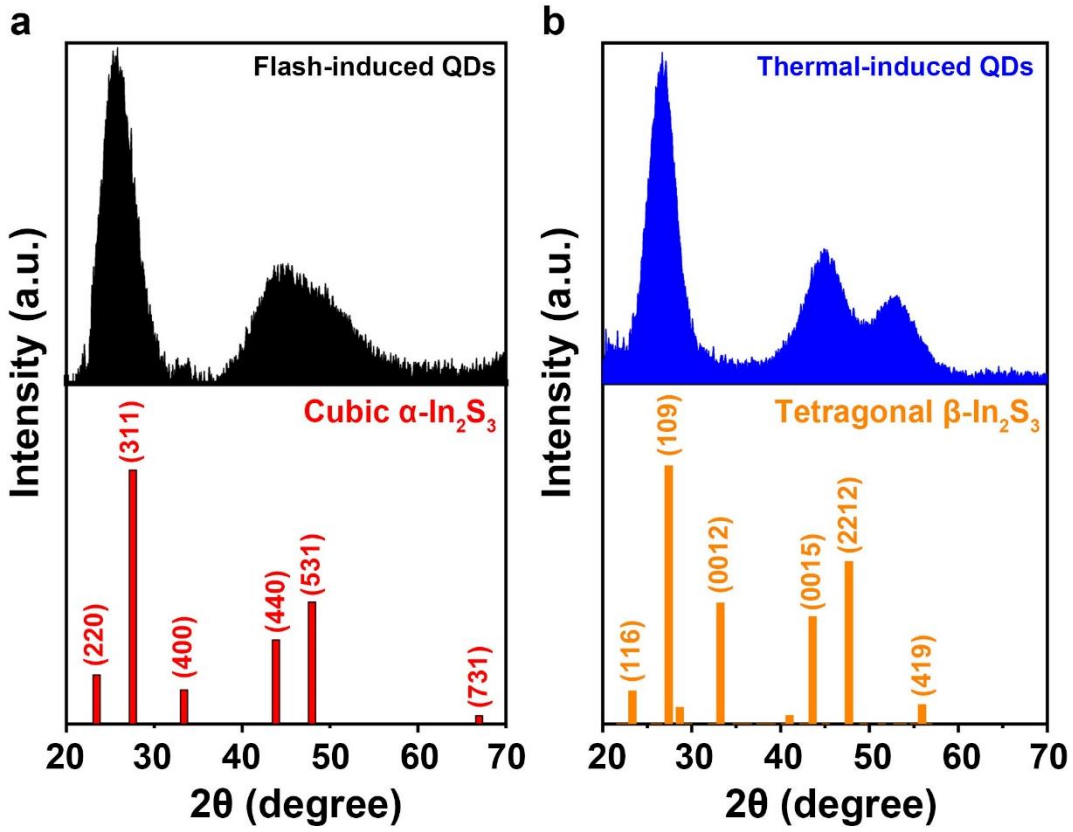

Fig. S9. (a) XRD pattern of light-induced metastable Ag, ZnS: α-In_2S_3 QDs presenting the cubic crystal structure (JCPDS No. 01-077-2729). (b) XRD peaks of conventional thermally synthesized β-In_2S_3 showing tetragonal structure (JCPDS No. 00-025-0390).

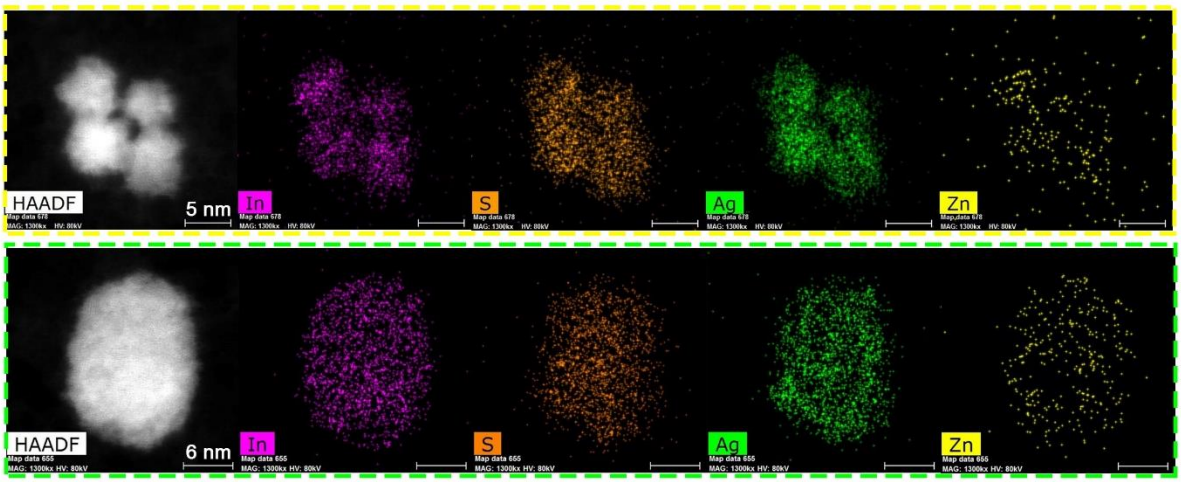

Fig. S10. Ripening and attachment of Ag, ZnS: α-In_2S_3 QDs via irradiation of more than 8 pulse on reaction solution (upper images for 10 pulses and lower images for 12 pulses). The ripening of QDs caused the degradation of optical performance.

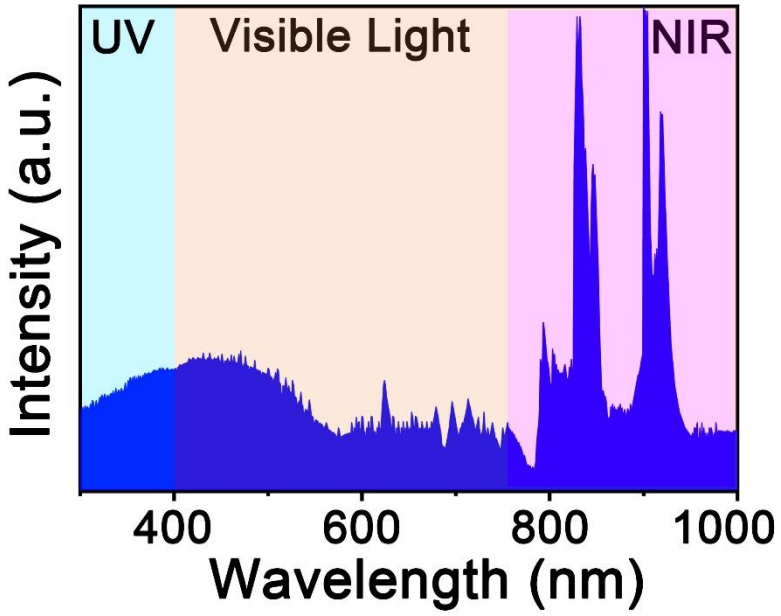

Fig. S11. Emission Spectrum of our xenon flash system from UV to NIR wavelength. The relatively high energy intensity of 400 nm and 850 nm were selected as optical excitation of light-induced QD synthesis in FDTD calculation.

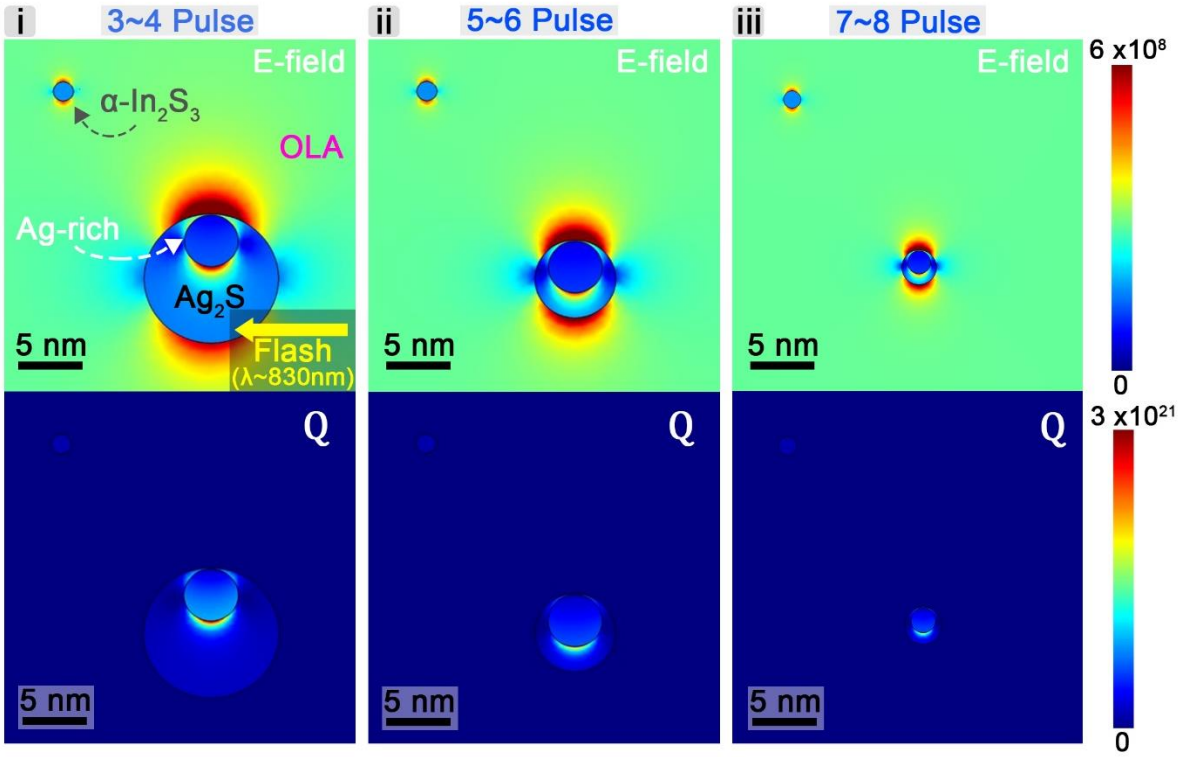

Fig. S12. E-field and Q calculation of silver sulfide NPs, metastable QD and OLA solvent via NIR electromagnetic wave absorption (λ ~ 830 nm). The size of silver sulfide was selected as i) 10 nm, ii) 6 nm, iii) 4 nm. The diameter of In_2S_3 QD was fixed with 3 nm.

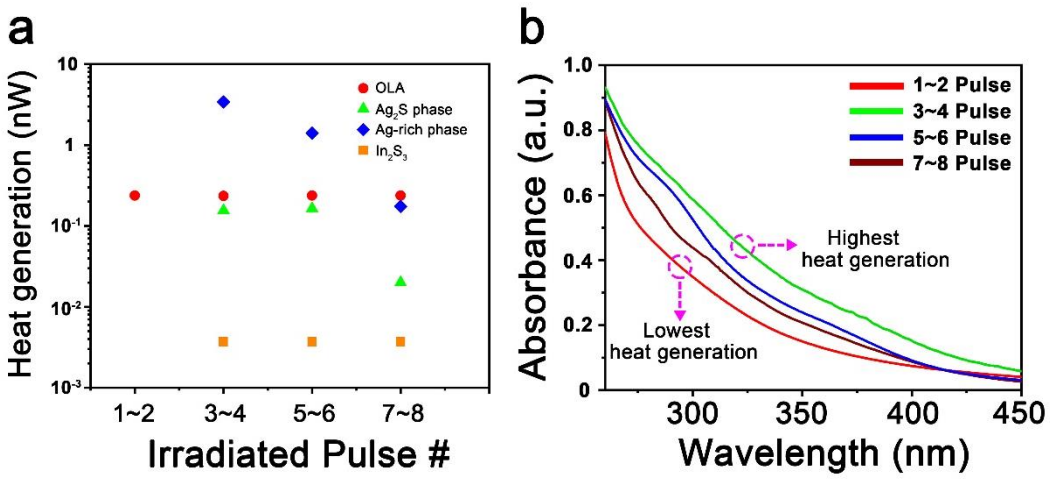

Fig. S13. (a) Theoretical heat generation of every substances including silver sulfide NPs, α-In_2S_3 QD according to the number of irradiated flash pulses on reaction solution. The highest heat generation was occurred at the stage of 3~4 pulse illumination. (b) Optical absorption spectra of reaction solution according to the multiple irradiation of flash pulses. The highest absorption of UV photon was occurred at the stage of 3 ~ 4 pulse illumination.

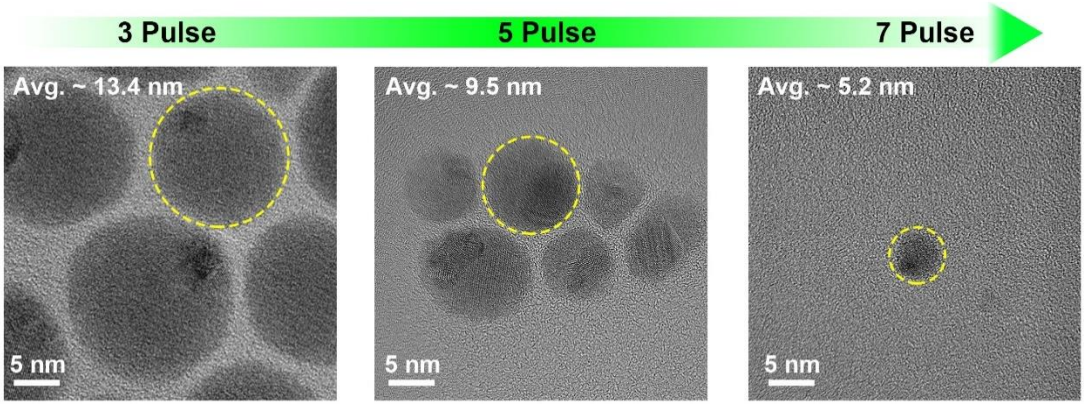

Fig. S14. Size decrement of intermediate Ag_2S/Ag NPs via the increased number of flash pulse illumination. The average size of NPs were decreased from maximum 13.4 nm to minimum 5.2 nm.

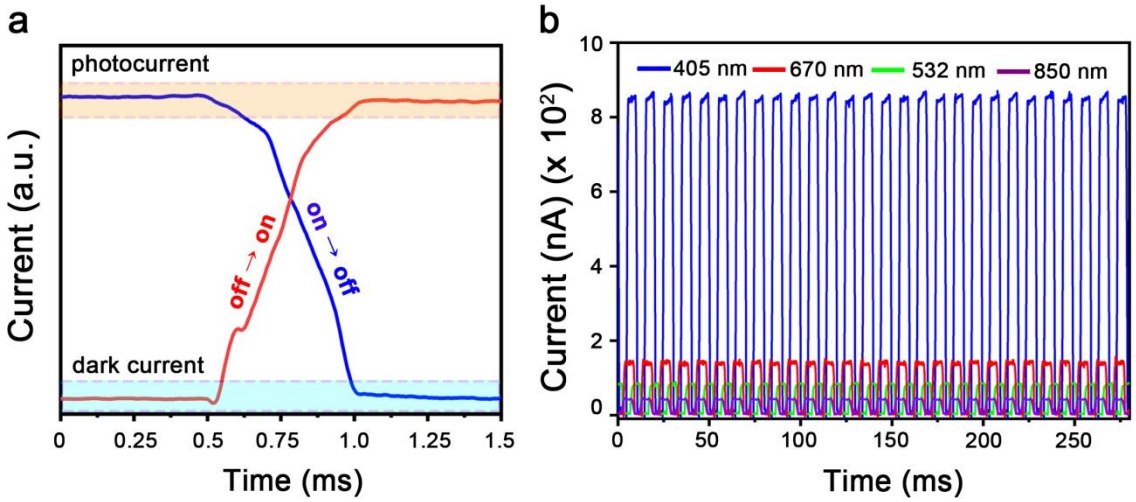

Fig. S15. (a) Magnified response speed of optoelectronic device via excitation of 532 nm wavelength. Both turn-on state (off → on) and turn-off state (on → off) presented response speed of ~ 500 μs. (b) Driving reliability of optoelectric device under excitation of 405, 532, 670 and 850 nm wavelength.

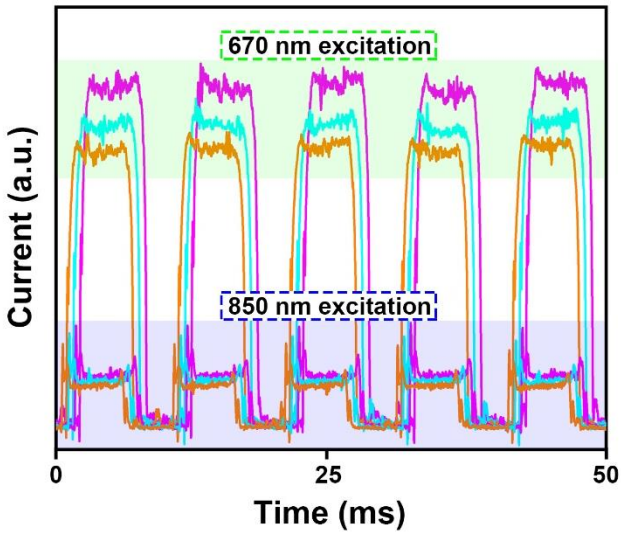

Fig. S16. Time-dependent optical response of a photoelectric device with excitations of 670 nm and 850 nm after 2 and 6 months. The purple graph is the photocurrent of as-prepared device. The photocurrent measured after 2 month (cyan graph) and 6 months (orange graph) presented almost same degree of photocurrent degradation in case of 405 nm and 532 nm.

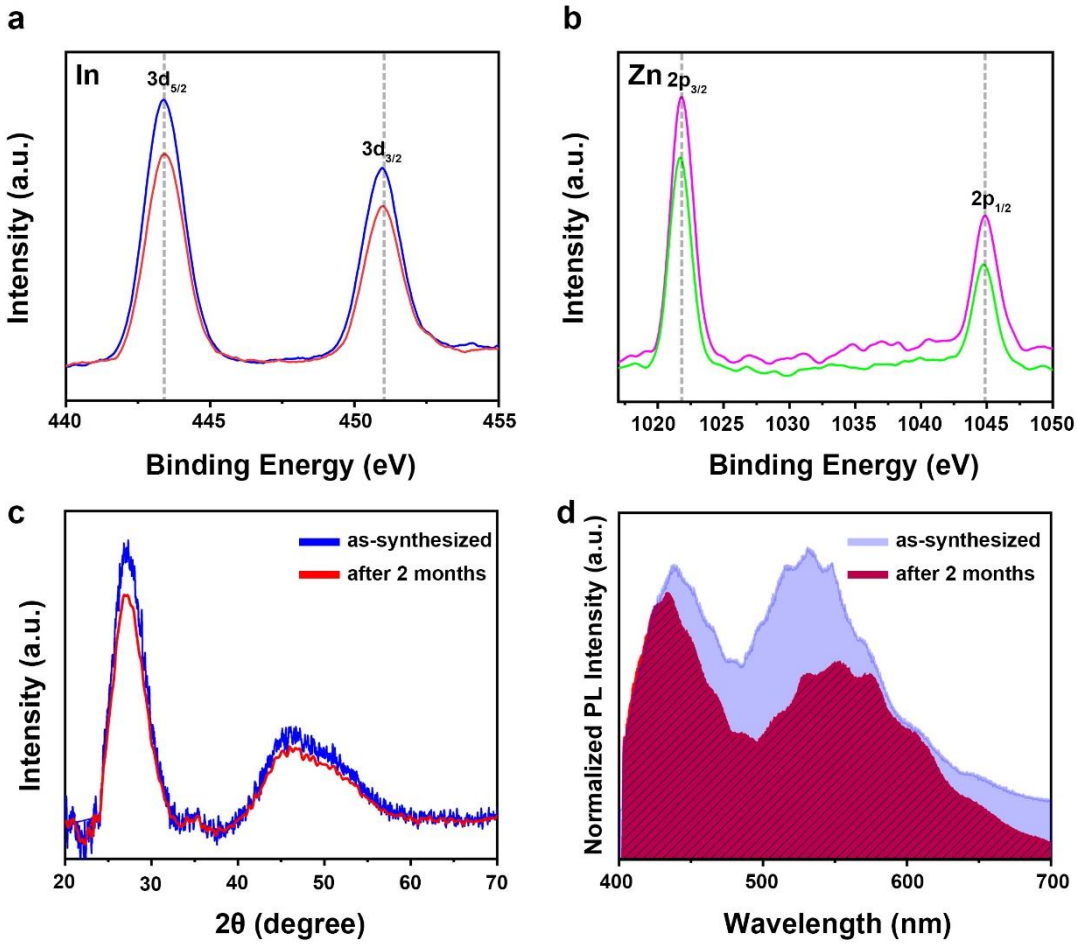

Fig. S17. (a) XPS In peaks of as-synthesized metastable QDs (blue graph) and stored sample for 6 months (red graph). Only reduction of peak intensity was analyzed without peak shifts. (b) XPS Zn peaks of as-synthesized QDs (purple graph) and stored sample for 6 months (green graph). Zn peaks also presented reduction of peak intensity without shifts of binding energy. (c) Comparison of XRD data between as-synthesized QDs (blue graph) and stored sample for 2 months (red graph). (d) Comparison of PL spectra between as-synthesized QDs (blue graph) and stored for 2 months (red graph).

	Thermal Conductivity (W/m*K)	Heat Capacity (J/kg*K)	Density (kg/m^3)	Molar Mass (g/mol)	Supporting References
In_2S_3 NPs	4	146.70	5180	325.831	[S2, S3]
Ag_2S phase	0.9	76.57	7234	247.8	[S4, S5]
Ag phase	419	240	10500	107.86	[S6]
Oleylamine	0.175	2215	813	267.493	[S7]

Table S1. Input physical properties of each material for FDTD calculation.

Samples	τ_1(ns)	τ_2(ns)	τ_3(ns)	τ_{avg}(ns)	χ^2
4 Pulse	17.8	77.9	180.6	112.3	1.05
5 Pulse	34.6	151.7	362.6	231.2	1.01
6 Pulse	36.4	164.6	392.0	255.3	1.17
8 Pulse	44.5	198.9	470.8	301.5	1.03

Table S2. Decay components and average photon lifetime of the metastable QDs according to the number of irradiated flash pulses.

Supporting Information References

[S1] Sadovnikov, S.; Gusev, A.; Rempel, A., Nonstoichiometry of nanocrystalline monoclinic silver sulfide. Phys. Chem. Chem. Phys. 17 (2015) 12466-12471

[S2] Nishino, T.; Hamakawa, Y., Preparation and properties of InS single Crystals. Japanese Journal of Applied Physics. 16 (1977) 1291-1300

[S3] Werheit, H.; Schmechel, R., Numerical data and functional relationships in science and technology Group III. 4 (1998) 3

[S4] Patnaik, P., Handbook of Inorganic Chemicals. The McGraw-Hill Companies. 2003 p.845

[S5] Lide, D., CRC handbook of chemistry and physics. CRC Press: Boca Raton, FL. 2004

[S6] Pileni, M., Fabrication and physical properties of self-organized silver nanocrystals. Pure and applied chemistry. 72 (2009) 53-65

[S7] Mourdikoudis, S.; Liz-Marzán, L. M., Oleylamine in nanoparticle synthesis. Chemistry of Materials. 25 (2013) 1465-1476